Published in final edited form as:
Mol Pharmacol. 2008 January ; 73(1): 243–251. doi:10.1124/mol.107.039594.

Disruption of cAMP and Prostaglandin E_2 Transport by Multidrug Resistance Protein 4 Deficiency Alters cAMP-Mediated Signaling and Nociceptive Response

Z. Ping Lin[1], **Yong-Lian Zhu**[1], **Dennis R. Johnson**[1], **Kevin P. Rice**[4], **Timothy Nottoli**[2], **Bryan C. Hains**[3], **James McGrath**[2], **Stephen G. Waxman**[3], and **Alan C. Sartorelli**[1]

[1] Department of Pharmacology and Developmental Therapeutics Program, Yale University School of Medicine, New Haven, Connecticut

[2] Section of Comparative Medicine, Yale University School of Medicine, New Haven, Connecticut

[3] Cancer Center, and Department of Neurology, Yale University School of Medicine, New Haven, Connecticut

[4] Department of Chemistry, Colby College, Waterville, Maine

Abstract

Multidrug resistance protein 4 (MRP4; ABCC4) is a member of the MRP/ATP-binding cassette family serving as a transmembrane transporter involved in energy-dependent efflux of anticancer/antiviral nucleotide agents and of physiological substrates, including cyclic nucleotides and prostaglandins (PGs). Phenotypic consequences of mrp4 deficiency were investigated using mrp4-knockout mice and derived immortalized mouse embryonic fibroblast (MEF) cells. Mrp4 deficiency caused decreased extracellular and increased intracellular levels of cAMP in MEF cells under normal and forskolin-stimulated conditions. Mrp4 deficiency and RNA interference-mediated mrp4 knockdown led to a pronounced reduction in extracellular PGE_2 but with no accumulation of intracellular PGE_2 in MEF cells. This result was consistent with attenuated cAMP-dependent protein kinase activity and reduced cyclooxygenase-2 (Cox-2) expression in mrp4-deficient MEF cells, suggesting that PG synthesis is restrained along with a lack of PG transport caused by mrp4 deficiency. Mice lacking mrp4 exhibited no outward phenotypes but had a decrease in plasma PGE metabolites and an increase in inflammatory pain threshold compared with wild-type mice. Collectively, these findings imply that mrp4 mediates the efflux of PGE_2 and concomitantly modulates cAMP mediated signaling for balanced PG synthesis in MEF cells. Abrogation of mrp4 affects the regulation of peripheral PG levels and consequently alters inflammatory nociceptive responses in vivo.

MRP4 (ABCC4) is a member of the multidrug resistance proteins (MRPs) belonging to the C group of the ATP-binding cassette (ABC) protein superfamily. To date, nine total MRP members, MRP1 (ABCC1), MRP2 (ABCC2), MRP3 (ABCC3), MRP4 (ABCC4), MRP5 (ABCC5), MRP6 (ABCC6), MRP7 (ABCC10), MRP8 (ABCC11), and MRP9 (ABCC12), have been identified. MRP4 functions as an energy-dependent, transmembrane efflux transporter closely related to three other MRP family members, MRPs 5, 8, and 9, with respect to structure and functional characteristics (Kruh and Belinsky, 2003; Deeley et al., 2006). Based

Address correspondence to: Alan C. Sartorelli, Department of Pharmacology, Yale University School of Medicine, 333 Cedar St., New Haven, CT 06520. alan.sartorelli@yale.edu.
Z.P.L., Y.-L.Z., and D.R.J. contributed equally to this work.

Article, publication date, and citation information can be found at http://molpharm.aspetjournals.org.

upon predicted membrane topology, MRPs 4, 5, 8, and 9 consist of a cytoplasmic segment (L_0) and a P-glycoprotein-like core structure but lack the NH_2-terminal domain (TMD_0) that is present in all of the other MRPs (Kruh and Belinsky, 2003; Deeley et al., 2006). MRPs 1, 2, 3, and 4 function physiologically as organic anion transporters mediating the efflux of glutathione, glucuronate, and sulfate conjugates whereas MRP5 does not (Kruh and Belinsky, 2003; Deeley et al., 2006).

Both MRPs 4 and 5 are capable of transporting cAMP and cGMP (Jedlitschky et al., 2000; Chen et al., 2001), the cyclic nucleotides that play critical roles in intracellular signaling. This unique transport capacity also led to the findings that MRPs 4 and 5 mediate the efflux of purine nucleotide analogs derived from the anticancer 6-thiopurines and of the antiviral purine nucleotide analog 9-(2-phosphonylmethoxyethyl)adenine (PMEA; Adefovir) (Schuetz et al., 1999; Wijnholds et al., 2000; Chen et al., 2001). MRP8 (ABCC11) has recently been shown to also transport cAMP and cGMP, as well as purine and pyrimidine nucleotide analogs (Guo et al., 2003; Chen et al., 2005). In the mouse, however, there is no ortholog for MRP8 (Shimizu et al., 2003; Maher et al., 2005). Although the functions of mrp9/MRP9 (abcc12/ABCC12) are currently undefined, this transporter is extensively distributed in various human tissues but is expressed only in mouse testis (Shimizu et al., 2003; Maher et al., 2005). Thus, the transport of physiological substrates by mrp4 and mrp5 is less likely to be influenced by mrp8 or mrp9 in the mouse.

The cyclic nucleotides and prostaglandins (PG) E_1 and E_2 are among several physiological substrates identified as being transported by MRP4 (Reid et al., 2003; Sauna et al., 2004; Rius et al., 2005). The cyclic nucleotides are well-characterized physiological molecules with pivotal roles in cellular communication and signaling. cAMP functions as an intracellular second messenger that mediates a broad range of cellular responses by activation of cAMP-dependent protein kinase (PKA) (Mayr and Montminy, 2001). The activation of PKA involves the binding of cAMP to regulatory subunits and the subsequent dissociation and nuclear translocation of catalytic subunits. Nuclear-localized catalytic subunits mediate the phosphorylation of the cAMP-response element (CRE)-binding protein (CREB) at Ser133, which promotes the transcription of a variety of target genes (Mayr and Montminy, 2001).

Two isoforms of cyclooxygenases (Cox) are required for catalyzing the synthesis of PGs from arachidonic acid. Cox-1 is constitutively expressed in most tissues, whereas Cox-2 is rapidly induced in response to mitogens, growth factors, and inflammatory cytokines (Smith et al., 2000). The Cox-2 gene contains a consensus CRE motif, TGACGTCA, in its promoter sequences and is one of many genes transcriptionally targeted by the cAMP-dependent signaling pathway (Mayr and Montminy, 2001). The induction of Cox-2 is responsible for an increase in the production of PGE_2, a primary PG involved in hyperalgesia through enhancing nociceptive effects of inflammatory mediators at the site of inflammation (Burian and Geisslinger, 2005). Therefore, inhibition of Cox-mediated PG synthesis is broadly accepted as the primary mechanism for the antinociceptive effects of nonsteroidal anti-inflammatory drugs (NSAIDs).

In the present study, the functional importance of mrp4, the murine ortholog of MRP4, in the transport of cAMP and PGE_2 was investigated through establishment of mice with a homozygous disruption of the *mrp4* gene. The involvement of mrp4 in the efflux transport of PGs and the cAMP-mediated signaling pathway was also explored with immortalized embryonic fibroblast cell lines established from *mrp4*-deficient mice. Through behavioral analyses of gene knockout animals, a phenotypic consequence of the *mrp4* deficiency involving altered inflammatory nociceptive response was also elucidated. The findings demonstrate that mrp4 contributes to the transport of PGs and the regulation of the cAMP-mediated signaling pathway leading to PG synthesis.

Materials and Methods

Generation and Breeding of Mrp4-Null (*Mrp*$^{-/-}$) Mice

The embryonic stem cell line RR212 (strain 129P2/Ola Hsd) containing a heterozygous gene trap disruption of the *abcc4* gene was obtained from BayGenomics/Multiple Myeloma Research Consortium (MMRC) (University of California Davis, Davis, CA). Chimeras were generated from this cell line by standard blastocyst microinjection and embryo transfer by the Animal Genomics Services at the Yale University School of Medicine (New Haven, CT). High percentage male chimeras were mated with C57BL/6 female mice (Charles River, Wilmington, MA), and agouti F1 offspring were genotyped using PCR analyses for the presence of the neomycin sequence (see *Genotyping*). Positive, *mrp4*$^{+/-}$ F1 mice were subsequently mated to yield F2 animals with homozygous disruption of the *mrp4* gene (*mrp4*$^{-/-}$).

Genotyping

Tail DNA was purified using the Puregene Genomic DNA Purification Kit (Gentra Systems, Minneapolis, MN) according to the manufacturer's instructions. Initial PCR neomycin cassette-based genotyping of the F1 heterozygotes was conducted according to the protocol of BayGenomics/MMRC using the neomycin sequence forward primer 5′-CTTGGGTGGAGAGGCTATTC-3′ and the reverse primer 5′-AGGTGAGATGACAGGAGATC-3′. Subsequent genotyping was directed at unique wild-type and knockout alleles by Southern blot and/or PCR analyses. NCBI-BLAST genomic DNA homology searching placed the 5′-rapid amplification of cDNA ends *mrp4* sequence of the RR212 ES clone within the *Mus musculus* clone RP24–212C1 (AC122778). AC122778 contains EcoRV restriction sites at positions 21258 and 38757, yielding a 17.5-kb wild-type band on Southern blotting. Gene trap insertion of the disrupting vector sequence (pGT1lxf; BayGenomics) between the wild-type EcoRV sites of AC122778 introduced a third EcoRV site yielding a diagnostic 11.5-kb knockout allele. Hybond-N+ membrane (GE Healthcare, Chalfont St. Giles, Buckinghamshire, UK) blots of EcoRV digested genomic DNA (15 μg) were probed with a ^{32}P-labeled 514-bp PCR generated probe, located 5′ to the disrupted intronic sequence of AC122778. The probe was prepared by amplifying the sequence of AC122778 corresponding to position 21752 through 22266 with the forward/reverse primer pair 5′-TAGGGTGAGATGGTGCAG-3′/5′-CCTTAGATTTGCCTGTGG-3′. Subsequently, all genotyping was performed by PCR using a cocktail of three primers: 5′-TCCATGAGACATGCATTGAGTGACT-3′ (wild-type forward), 5′-GAACACCAGTAGGGATCTCGCTAT (wild-type reverse), and 5′-ATGAGATGGATTGGCAGATGTAGCT-3′ (knockout reverse) under the conditions of one cycle of 95°C for 2 min, followed by 35 cycles of 95°C for 1 min, 63°C for 1 min, 72°C for 1 min, and finally one cycle of 72°C for 7 min. The PCR reaction yielded a 582-bp wild-type product and a 220-bp knockout product. Sequence analysis of the knockout PCR product localized the insertion of the disrupting vector sequence to the intronic sequence of AC122778 immediately 3′ to nucleotide 25950, with the most 5′ portion of the disrupting vector, pGT1lxf, being nucleotide 1196 of the En2 sequence.

Generation and Immortalization of Primary Embryonic Fibroblasts

Mrp4$^{+/+}$ and *mrp4*$^{-/-}$ primary embryonic fibroblasts were generated by pairing heterozygous *mrp4*$^{+/-}$ parents, followed by harvesting embryos on days 14.5 to 15.5 and genotyping. The pregnant dam was euthanized by carbon dioxide asphyxiation and swabbed with 70% ethanol, and the uterus was removed. The 12 embryos within were individually minced with a sterile razor blade, incubated with trypsin/EDTA, dissociated, and cultured in dishes containing Dulbecco's modified Eagle's medium supplemented with 10% fetal bovine serum, penicillin, and streptomycin. Fibroblasts were frozen at passage 2. The procedure for transfection and immortalization of primary embryonic fibroblast cells was described previously (Lin et al.,

2002) with some modification. In brief, primary embryonic fibroblast cells were cotransfected with pCC2pA and pCMV-Bsd plasmids. At 48 h after transfection, 4 μg/ml of Blasticidin S (Invitrogen, Carlsbad, CA) was added for 10 days to select resistant colonies. The total population of resistant colonies was pooled for each of the *mrp4*$^{+/+}$ and *mrp4*$^{-/-}$ fibroblasts, which were continuously cultured in the presence of Blasticidin S for another month and expanded into immortalized cell lines.

RT-PCR Analysis

Total RNA was isolated using an RNeasy kit (QIAGEN, Valencia, CA) according to the manufacturer's protocol. Primer sequences of wild-type mrp4 (AY415508) for RT-PCR were forward 5′-TGTGCTGCTTAACATGGTGG-3′ and reverse 5′-GCAAATCATCCATGTGTCCG-3′. For the knockout mrp4/β-geo (β-galactosidase-neomycin fusion) RT-PCR reaction, the same forward primer for wild-type mrp4 and a reverse primer 5′-TCCCAGTCACGACGT-TGTAA-3′, corresponding to the sequence of pGT1lxf vector from position 1645 through 1664, were used. Primer sequences of murine mrp1, mrp5, and β-actin and RT-PCR conditions used were described previously (Lin et al., 2002).

Cytotoxicity Assay

The sensitivity of immortalized fibroblasts to PMEA (Moravek, Brea, CA; Gilead, Foster City, CA) was determined by the MTS cytotoxicity assay as described previously (Lin et al., 2002).

cAMP-dependent Protein Kinase Assay

Cell pellets were re-suspended in ice-cold PKA extraction buffer (25 mM Tris-HCl, 0.5 mM EDTA, 0.5 mM EGTA, 10 mM β-mercaptoethanol, 0.5 mM PMSF, and proteinase inhibitor cocktail; Roche, Indianapolis, IN), sonicated, and centrifugated to clear the lysates. Aliquots of lysates were used to measure protein concentrations by the Bio-Rad detergent-compatible protein assay (Bio-Rad Laboratories, Hercules, CA) according to the manufacturer's instructions. PKA activity was determined using the SignaTECT cAMP-dependent protein kinase assay system (Promega) as follows. Five microliters of cell lysate was added to 20 μl of a reaction cocktail (40 mM Tris-HCl, pH 7.4, 20 mM $MgCl_2$, 0.1 mg/ml bovine serum albumin, and 100 μM ATP, including 0.5 Ci/mmol [γ^{32}P]ATP and 100 μM biotinylated Kemptide substrate). The positive control reaction included 1 μM cAMP. Negative control reactions consisted of either substituted cell extraction buffer for cell lysates or included the PKA inhibitor protein PKI[5–24] (Promega, Madison, WI). Kinase reactions were incubated at 25°C for 5 min and then terminated with 0.5× volume of 7.5 M guanidine-HCl. Ten microliters of stopped reactions were applied to a streptavidin-coated membrane. Unbound labeled substrates were washed from the membrane four times with 200 ml of 2 M NaCl, then four times with 200 ml of 2 M NaCl in 1% H_3PO_4, and finally 2 times with 100 ml of deionized water; the membrane was then dried using a gel dryer. To determine the specific activity, 2 μl of terminated reactions were applied onto a membrane without washing; membranes were then exposed to a PhosphorImager screen. The intensities of spots were quantified and processed using ImageQuant software (GE Healthcare).

cAMP Enzyme Immunoassay

Cells were seeded into 6-well plates at 4×10^5 cells/well in 1 ml of complete medium and grown for 26 h. The medium was then collected and processed directly for measurement of extracellular cAMP levels. The cell monolayer was rinsed twice with ice-cold PBS and then incubated with 0.3 ml of 0.1 M HCl for 20 min at room temperature. The cells were then scraped, collected, and pipetted up and down until the lysate became homogeneous. The lysate was centrifuged and the supernatant was transferred for determination of intracellular cAMP

levels using a cyclic AMP EIA kit (Cayman Chemical, Ann Arbor, MI) according to the manufacturer's instructions.

PGE_2 Enzyme Immunoassay

Cells were seeded into six-well plates at 4×10^5 cells/well in 1 ml of complete medium, and grown in the presence or absence of drugs for 26 h. The medium was then collected and processed for measurement of extracellular PGE_2 levels. The cell monolayer was rinsed twice with ice-cold PBS and collected by scraping into 1 ml of ice-cold PBS. Cells were pelleted and stored at −80°C before the purification of intracellular PGE_2. Duplicate sets of samples were also saved for determination of cellular protein concentrations. Purification of intracellular PGE_2 was accomplished using C-18 Amprep minicolumns (GE Healthcare). Frozen cell pellets were taken up in 1 ml of homogenization buffer (0.1 M phosphate, pH 7.4, containing 1 mM EDTA, and 10 μM indomethacin), and then sonicated briefly three times in 3-s bursts. An aliquot of each sample was spiked with PGE_2 (20 pg) before purification for monitoring the recovery rate. After the addition of 1 ml of acetone, the samples were vortexed, allowed to stand for 20 min, and centrifuged at 25°C for 10 min; the acetone was then evaporated under a gentle stream of nitrogen. The pH of the samples was adjusted to 4.0 using 1 N HCl and the C-18 columns were activated before the addition of sample with 1 ml of methanol and 2 ml of water. After the addition of sample, the columns were washed with 1 ml of water followed by 1 ml of hexanes and the PGE_2 was eluted with 1 ml of ethyl acetate containing 1% methanol. The samples were subsequently dried under a gentle stream of nitrogen for the ELISA PGE_2 determinations. Both extracellular and intracellular PGE_2 were measured using the prostaglandin E_2 EIA kit (Cayman Chemical, Ann Arbor, MI) according to the manufacturer's instructions.

Measurement of Plasma PGE Metabolite

Mice were euthanized by CO_2 asphyxiation, and at least 500 μl of blood were immediately obtained and transferred into a tube containing EDTA (Microtainer; BD Biosciences, Franklin Lakes, NJ). The tubes were centrifuged and 25 μl of supernatant containing plasma was transferred to a tube in which 7.5 μl of carbonate buffer (Cayman Chemical, Ann Arbor, MI) was added. The plasma was then incubated at 37°C for 24 h. Thereafter, 10 μl of phosphate buffer and 7.5 μl of EIA buffer (Cayman Chemical) were added to the plasma, which was processed for measurement of PGEM using the Prostaglandin E Metabolite EIA kit (Cayman Chemical) according to the manufacturer's instructions.

Western Blot Analysis

The procedures were as described previously (Lin et al., 2002). Anti-mrp4 (M4I-10) antibody was obtained from Abcam (Cambridge, MA). Anti-mrp5 (C-17), Cox-2 (C-20), and Cox-1 (H-62) antibodies were purchased from Santa Cruz Biotechnology (Santa Cruz, CA). Anti-actin antibody was supplied by Sigma-Aldrich (St. Louis, MO).

Generation of sh/siRNA and Transient Transfections

Mouse mrp4 shRNAs were derived from the 19-base sequence of mouse mrp4 cDNAs CCACAGGCCAGATAGTTAA and CCTCGGCCTTAACAATATT (666–684 and 4041–4059, respectively, GenBank accession number NM_001033336). The control shRNA was a nontargeting sequence shRNA as described previously (Lin et al., 2007). shRNA was generated by in vitro transcription using a MessageMuter shRNAi production kit (Epicenter, Madison, WI) according to methods published previously by our laboratory (Lin et al., 2007). Cells were plated in six-well plates, incubated for 24 h, and transfected with 50 nM shRNA using a Lipofectamine 2000 transfection reagent (Invitrogen) according to the manufacturer's protocol. Transfected cells were incubated for the appropriate times before assays.

Determination of Inflammatory Pain Thresholds

Behavioral analyses were performed to assess mechanical and thermal nociceptive thresholds in a model of inflammatory pain. *Mrp4*$^{-/-}$ mice and control *mrp4*$^{+/+}$ mice were exposed to 50 μl of a 3% capsaicin solution in 30% DMSO by intradermal injection into the glabrous surface of the hind paw using 3% halothane anesthesia. After acclimation to the testing area (30 min), mechanical sensory thresholds were determined by paw withdrawal from the application of a series of von Frey filaments (Stoelting, Wood Dale, IL) to the glabrous surface of the paw. After application of calibrated von Frey filaments (0.4–26 g, verified by calibration against a force transducer) with enough force to cause buckling of the filament, a modification of the "up-down" method of Dixon (1980) was used to determine the value at which paw withdrawal occurred 50% of the time (Chaplan et al., 1994), interpreted to be the mechanical nociceptive threshold.

After acclimation to the test chamber, thermal hyperalgesia was assessed by measuring the latency of paw withdrawal in response to a radiant heat source (Dirig et al., 1997). Mice were placed in Plexiglas boxes on an elevated glass plate under which a radiant heat source (4.7 amps) was applied to the glabrous surface of the paw through the glass plate. The heat source was turned off automatically by a photocell upon limb-lift, allowing the measurement of paw withdrawal latency. Three min was allowed between each trial, and 4 trials were averaged for each limb.

Results

Homozygous Disruption of Mrp4 in Mice and MEFs

The *mrp4* gene was disrupted by a GeneTrap vector through an insertional mutation in the intron sequence between exons 18 and 19. As a result, the normal transcript processing of *mrp4* mRNA was interrupted by the exon of the *β-geo* gene from the inserted GeneTrap vector (Fig. 1A). Disruption of both alleles of the *mrp4* gene was confirmed by Southern blotting (Fig. 1B) and PCR analysis (Fig. 1C) of tail genomic DNA. Mice containing homozygous disruption of the *mrp4* gene bred normally and did not display an outward phenotype appreciably different from their wild-type counterparts (data not shown).

Immortalization of *mrp4*$^{+/+}$ and *mrp4*$^{-/-}$ primary embryonic fibroblasts derived from these mice was carried out by the previously described method of stable transfection with the simian virus 40 large T antigen (Lin et al., 2002). Abrogation of *mrp4* expression at the mRNA level by the GeneTrap vector was confirmed by RT-PCR analyses for these immortalized cell lines. Using primers corresponding to the sequences in exons 16 and 20 of *mrp4*, a predicted 356-bp RT-PCR product was amplified in *mrp*$^{+/+}$ MEF cells but not in *mrp4*$^{-/-}$ MEF cells (Fig. 1D). Because the disruption by the GeneTrap vector resulted in *β-geo* sequences joined to the exon sequences of *mrp4* after exon 18 (Fig. 1A), a predicted 290-bp, mrp4-*β*-geo fusion PCR product was amplified only in *mrp4*$^{-/-}$ MEF cells when the same forward primer of wild-type *mrp4* and a reverse primer of the *β-geo* gene in the vector were used. RT-PCR products for mrp1, mrp5, and *β*-actin mRNA were amplified at comparable levels among *mrp4*$^{+/+}$ and *mrp4*$^{-/-}$ MEF cells. Furthermore, a complete elimination of mrp4 protein was also verified in *mrp4*$^{-/-}$ MEF cells by Western blot analysis (Fig. 1E). The level of mrp5 protein in *mrp4*$^{-/-}$ MEF cells remained similar to that of *mrp4*$^{+/+}$ MEF cells.

Augmentation of PMEA Cytotoxicity and Intracellular cAMP Levels in Mrp4-Deficient MEF Cells

MRP4 reportedly serves as a high-affinity transporter for the nucleotide analog PMEA, and overexpression of MRP4 has been shown to confer resistance to the cytotoxicity of PMEA (Schuetz et al., 1999; Lee et al., 2000). To determine the effects of *mrp4* abrogation on the

sensitivity of cells to PMEA, the cytotoxicity of this agent to MEF cells after 72 h of exposure was determined by the MTS cytotoxicity assay. *Mrp4*$^{-/-}$ MEF cells exhibited a marked increase (10-fold) in sensitivity to PMEA compared with *mrp4*$^{+/+}$ MEF cells (Fig. 2A). In contrast, both MEF cell lines exhibited similar sensitivity to vinblastine, a cytotoxic agent that is not transported by mrp4 (Fig. 2B). We have also found that treatment with MK-571, an inhibitor of mrp4 (Chen et al., 2002), partially sensitized *mrp4*$^{+/+}$ MEF cells to PMEA (data not shown). These results are consistent with a recent report of independently developed mrp4-deficient mice (Belinsky et al., 2007) and indicate that the loss of mrp4 augments the cytotoxicity of PMEA as a result of a decrease in efflux of this agent in *mrp4*$^{-/-}$ MEF cells.

Using models of overexpressing cell lines and/or membrane vesicles, MRP4 has been demonstrated to mediate the efflux of cAMP (Chen et al., 2001; Wielinga et al., 2003). To corroborate this phenomenon with cells deficient in mrp4, we measured the levels of extracellular and intracellular cAMP in MEF cells stimulated with forskolin (FSK), an activator of adenylate cyclase that induces a rapid elevation of the intracellular cAMP level (Seamon et al., 1981). Exposure to FSK for 1 h caused a significant increase in extracellular and intracellular cAMP levels in both *mrp4*$^{+/+}$ and *mrp4*$^{-/-}$ MEF cells (Fig. 2C). The FSK-induced increase in the level of extracellular cAMP in *mrp4*$^{+/+}$ MEF cells was significantly greater than that occurring in *mrp4*$^{-/-}$ MEF cells. The lower basal and stimulated levels of extracellular cAMP in *mrp4*$^{-/-}$ MEF cells may be produced by the efflux activity of mrp5 (Jedlitschky et al., 2000). In contrast, exposure to FSK produced a significantly greater increase in the level of intracellular cAMP in *mrp4*$^{-/-}$ MEF cells than that occurring in *mrp4*$^{+/+}$ MEF cells. The basal level of intracellular cAMP in *mrp4*$^{-/-}$ MEF cells was significantly higher than that in *mrp4*$^{+/+}$ MEF cells. These findings suggest that the disruption of mrp4 reduces the efflux of cAMP and therefore leads to an elevated level of intracellular cAMP under normal and stimulated conditions.

Effects of Mrp4 Deficiency on PKA Activity and Cox-2 Expression

The activity of PKA is modulated by changes in the intracellular level of cAMP. Therefore, we determined whether mrp4 deficiency had effects on basal and stimulated PKA activity in MEF cells. To further augment cAMP levels and PKA activity, 3-isobutyl-1-methylxanthine (IBMX), a broad-spectrum phosphodiesterase inhibitor that blocks the hydrolysis of cAMP (Chasin and Harris, 1976), was also used in combination with FSK. *Mrp4*$^{-/-}$ MEF cells exhibited a significant decrease in basal PKA activity (~50%) relative to *mrp4*$^{+/+}$ MEF cells (Fig. 3A). Treatment with IBMX alone for 1 h had minimal effect on basal PKA activity but augmented FSK-stimulated PKA activity in both *mrp4*$^{+/+}$ and *mrp4*$^{-/-}$ MEF cells. Exposure to FSK or FSK in combination with IBMX for 1 h seemed to cause an increase in PKA activity of greater magnitude in *mrp4*$^{-/-}$ MEF cells compared with that occurring in *mrp4*$^{+/+}$ MEF cells. These findings indicate that PKA activity responds to a rapid change in the intracellular level of cAMP stimulated by FSK treatment. In addition, the basal and overall PKA activities are attenuated in mrp4-deficient cells, possibly as a result of a prolonged accumulation of intracellular cAMP.

Cox-2, a cAMP-responsive gene, contains a CRE in its promoter region (Mayr and Montminy, 2001). It has been reported that the basal expression of Cox-2 is regulated by CREB protein (Wardlaw et al., 2002; Pino et al., 2005). To determine whether the mrp4 deficiency had effects on Cox-2 expression, the protein levels of Cox-2 in MEF cells were determined by Western blot analysis. Consistent with PKA activity, *mrp4*$^{-/-}$ MEF cells displayed a reduction (>50%) in the basal level of Cox-2 protein compared with *mrp4*$^{+/+}$ cells (Fig. 3B). These results were also in agreement with a decrease in the transcriptional activity of CREB in *mrp4*$^{-/-}$ MEF cells as determined by luciferase reporter assay (data not shown). The levels of Cox-2 protein after treatment with the cAMP-modulating agents described in Fig. 3A for 6 h were also quantified.

Treatment of *mrp4*$^{+/+}$ and *mrp4*$^{-/-}$ MEF cells with FSK or FSK in combination with IBMX produced an increase in the levels of Cox-2 protein in a manner analogous to that of PKA activity (Fig. 3B). These findings suggest that the expression of Cox-2 is under the control of PKA activity and is also attenuated as a result of mrp4 deficiency in MEF cells.

To test whether the attenuation of the PKA activity and Cox-2 expression was caused by a constant increase in basal level of intracellular cAMP in mrp4-deficient cells, the level of Cox-2 protein after prolonged exposure of MEF cells to IBMX was determined by Western blot analysis (Fig. 3C). Treatment of *mrp4*$^{+/+}$ MEF cells with IBMX at all tested concentrations for 24 h had no effect on the level of Cox-2. In contrast, the same treatment produced a further decrease in Cox-2 levels in *mrp4*$^{-/-}$ MEF cells, presumably as a result of a lack of or a slowdown in the removal of accumulated intracellular cAMP by mrp4. This finding confirms that a persistent increase in intracellular cAMP is accountable for the attenuation of PKA activity and Cox-2 expression in mrp4-deficient cells.

Contribution of Cox-2 and Mrp4 to the Efflux of PGE_2 in MEF Cells

MRP4 has been shown to mediate the efflux of PGE_2, one of the primary prostaglandins secreted by cells, in an ATP-dependent manner (Reid et al., 2003; Sauna et al., 2004; Rius et al., 2005). To characterize the kinetics of mrp4-mediated prostaglandin transport and the effects of mrp4 deficiency, the time course of changes in extracellular and intracellular levels of PGE_2 in MEF cells was determined, PGE_2 levels being measured at 3, 8, and 24 h after cell plating. Extracellular PGE_2 rapidly reached the highest level at 3 h followed by a gradual decline between 8 and 24 h (Fig. 4A), with *mrp4*$^{+/+}$ MEF cells exhibiting a much greater increase in the level of extracellular PGE_2 than *mrp4*$^{-/-}$ cells over the time course of measurement. At 24 h, *mrp4*$^{+/+}$ MEF cells showed a moderate decline (39% of the highest level reached) in the level of extracellular PGE_2, whereas *mrp4*$^{-/-}$ MEF cells exhibited a greater reduction (62% of the highest level reached) in extracellular PGE_2. The kinetics of intracellular PGE_2 levels were similar to that of extracellular PGE_2 in *mrp4*$^{+/+}$ and *mrp4*$^{-/-}$ MEF cells (Fig. 4B). However, both *mrp4*$^{+/+}$ and *mrp4*$^{-/-}$ MEF cells exhibited a substantial reduction in the intracellular PGE_2 (~65% of the highest levels reached) at 24 h. To illustrate the contribution of mrp4 to the efflux of PGE_2, the ratios of extracellular PGE_2 to intracellular PGE_2 levels were calculated to correct for the differences in the intracellular PGE_2 level between *mrp4*$^{+/+}$ and *mrp4*$^{-/-}$ cells (Fig. 4C). The ratio for *mrp4*$^{+/+}$ MEF cells was higher than that of *mrp4*$^{-/-}$ cells and continued to rise with time, whereas the lower ratio for *mrp4*$^{-/-}$ cells reached a plateau at 3 h. At 24 h, the ratio for *mrp4*$^{+/+}$ MEF cells was significantly higher than that of *mrp4*$^{-/-}$ cells, suggesting that mrp4 contributes to the considerable level of extracellular PGE_2 in *mrp4*$^{+/+}$ MEF cells. The expression of Cox-2 protein in *mrp4*$^{+/+}$ and *mrp4*$^{-/-}$ MEF cells was also determined simultaneously with the PGE_2 measurements. *Mrp4*$^{+/+}$ MEF cells exhibited a greater induction of Cox-2 protein than *mrp4*$^{-/-}$ cells at each time point over the course of the measurements (Fig. 4D). The kinetics of Cox-2 induction corresponded closely to that of intracellular PGE_2 levels and both *mrp4*$^{+/+}$ and *mrp4*$^{-/-}$ MEF cells exhibited a substantial decline in Cox-2 protein levels at 24 h.

The contribution of cAMP-mediated signaling and Cox-2 to extracellular PGE_2 was also examined. Treatment of *mrp4*$^{+/+}$ MEF cells with H-89, a specific PKA inhibitor (Chijiwa et al., 1990), led to a partial decrease (53%) in the level of extracellular PGE_2 (Fig. 4E). Furthermore, treatment of *mrp4*$^{+/+}$ MEF cells with the Cox-2 preferential inhibitor 6-methoxy-2-naphthyl acetic acid (Meade et al., 1993) caused a marked reduction (88%) in the level of extracellular PGE_2. Both inhibitors produced a significant reduction in the level of extracellular PGE_2 produced by *mrp4*$^{+/+}$ cells but no significant effects on *mrp4*$^{-/-}$ MEF cells (one-way ANOVA). Taken together, these findings suggest that the level of extracellular

PGE_2 is attributable to the combination of mrp4-mediated efflux PGE_2 and cAMP signaling-modulated Cox-2 expression in MEF cells.

Effects of Mrp4 Knockdown by siRNA on the Extracellular and Intracellular Levels of PGE_2 in MEF cells

To provide further evidence that mrp4 was required for the efflux of PGE_2 in MEF cells, transient knockdown of mrp4 using RNA interference was carried out in *mrp4*$^{+/+}$ MEF cells. Transfection of *mrp4*$^{+/+}$ MEF cells with either of two different mrp4-siRNAs (1 and 2) caused partial but considerable knockdown of mrp4 concurrently with a relatively moderate reduction in Cox-2 (Fig. 5A). This concomitant reduction in Cox-2, albeit to a lesser extent, was consistent with that occurring in *mrp4*$^{-/-}$ MEF cells (Fig. 3B). Whether mrp4 knockdown in *mrp4*$^{+/+}$ MEF cells had effects on the transport of PGE_2 was investigated by measuring extracellular and intracellular levels of PGE_2. Transfection of *mrp4*$^{+/+}$ MEF cells with either of the mrp4-siRNAs resulted in a marked decrease (>70%) in the extracellular levels of PGE_2 (Fig. 5B). In contrast, the intracellular levels of PGE_2 were minimally affected by the knockdowns of mrp4 (Fig. 5C). These results corroborate the findings with mrp4 deficient MEF cells, indicating that mrp4 is responsible for the efflux of PGE_2 in MEF cells.

Plasma Levels of PGE Metabolite and Inflammatory Nociceptive Threshold in Mrp4-Deficient Mice

Because a marked reduction in the extracellular levels of PGE_2 occurred in *mrp4*$^{-/-}$ MEF cells relative to *mrp4*$^{+/+}$ MEF cells, we ascertained whether the genetic deficiency of mrp4 in mice affected the plasma levels of PGE_1 and PGE_2. Because of the rapid and extensive degradation in vivo, PGEM, the PGE_1 and PGE_2 metabolite present in the plasma, was measured to estimate the level of PGE_2 secreted into the extracellular fluids and the circulation. Plasma samples were collected from six to seven mice of each genotype. Consistent with the finding with MEF cells, *mrp4*$^{-/-}$ mice exhibited an approximate 50% decrease in the levels of PGEM in the plasma relative to wild-type animals (Fig. 6A).

Because PGE_1 and PGE_2 in the periphery enhance nociceptive pathways to produce hyperalgesia or pain hypersensitivity (Burian and Geisslinger, 2005), we measured whether mrp4 deficiency resulted in an altered responsiveness to pain in mice after a local inflammatory challenge. To accomplish this, wild-type and *mrp4*$^{-/-}$ mice were assessed for thermal and mechanical nociceptive thresholds after unilateral intradermal injection of capsaicin, a local irritant producing an inflammatory response. The ipsilateral hind-paws were injected with capsaicin, whereas contralateral hindpaws not injected with capsaicin were used as controls. Both wild-type and *mrp4*$^{-/-}$ mice had a similar latency of paw withdrawal, or baseline threshold, in thermal and mechanical responses without administration of capsaicin (Fig. 6, B and C). It is noteworthy that *mrp4*$^{-/-}$ mice exhibited a prolonged latency of withdrawal from a thermal source (Fig. 6B) and an increase in tolerance to weight application (Fig. 6C) in ipsilateral hindpaws compared with wild-type animals. These findings suggest that a deficiency in mrp4 causes an increase in the threshold of pain responsiveness possibly attributable to a reduction in peripheral PGE_1 and PGE_2 levels.

Discussion

The discovery of MRP4 as a transporter of cyclic nucleotides and prostaglandins has important implications in the homeostasis of these signaling molecules inside cells. The efflux properties of MRP4 for cAMP and cGMP provide an alternative or complementary mechanism to the phosphodiesterases as modulators of the intracellular concentration of these second messengers (Chen et al., 2001; Adachi et al., 2002). It has been proposed that MRP4 functions as an overload mechanism for exceedingly high levels of cAMP and is less likely to regulate

intracellular cAMP levels because of its relatively low affinity for cyclic nucleotides (Adachi et al., 2002; Borst et al., 2004). However, our results with MEF cell lines deficient in mrp4 demonstrate that a decrease in extracellular cAMP occurs concurrently with an increase in the intracellular level of this cyclic nucleotide under conditions of normal growth and upon stimulation of cAMP synthesis. These findings provide evidence that MRP4/mrp4 can play a role in the regulation of intracellular cAMP levels.

An increase in the level of intracellular cAMP as a result of a deficiency in mrp4 has a significant impact on cAMP-mediated signaling events. Our results demonstrate that abrogation of mrp4 leads to attenuated PKA activity and down-regulated Cox-2 expression in MEF cells. We also show that prolonged treatment with the phosphodiesterase inhibitor IBMX produces a further down-regulation of Cox-2 in *mrp4*$^{-/-}$ MEF cells. The down-regulation does not occur in wild-type MEF cells exposed to IBMX because mrp4 remains available to bring down any increase in the level of intracellular cAMP. It has also been reported that long-term exposure of cells to a cAMP agonist causes a loss of the C-subunit of PKA and attenuates CREB transcriptional activity as a result of dephosphorylation of CREB at Ser133 (Mayr and Montminy, 2001). Thus, the attenuation of cAMP-mediated signaling in mrp4-deficient cells represents the cellular adaptation to the persistent elevation in intracellular cAMP or acts as a negative feedback mechanism to prevent excessive stimulation of the expression of target genes such as Cox-2.

Our gene knockout and knockdown studies support previously reported findings with overexpressed MRP4 that mrp4 mediates the efflux of PGE_2 (Reid et al., 2003; Sauna et al., 2004; Rius et al., 2005). Thus, mrp4 deficiency leads to a pronounced decrease in the levels of extracellular PGE_2. Noticeably, *mrp4*$^{-/-}$ cells still exhibit the kinetics of extracellular PGE_2 levels essentially paralleling that of extracellular PGE_2 levels in wild-type MEF cells during the early time points of the measurements. This small rise in extracellular PGE_2 levels in *mrp4*$^{-/-}$ cells, which coincides with the induction of Cox-2 protein after cell plating, may result from outward passive diffusion (Schuster, 2002) or the action of unidentified PGE_2 efflux transporters. However, mrp2, which has also been identified to mediate active efflux of PGE_2 (deWaart et al., 2006), does not play a role in this case because its expression is not detectable in MEF cells (Lin et al., 2002). A decline in extracellular PGE_2 levels in both *mrp4*$^{+/+}$ and *mrp4*$^{-/-}$ cells at 24 h is attributable to the combined effects of the prostaglandin transporter-mediated influx (Schuster, 2002) and a decrease in Cox-2 expression.

The data on intracellular levels of PGE_2, however, contradicted the assumption that an increase in intracellular PGE_2 would occur in the absence of the mrp4 transporter. In fact, the level of intracellular PGE_2 in mrp4-deficient cells is low, at approximately half that in *mrp4*$^{+/+}$ cells. We postulate that this phenomenon is attributable to an increase in the intracellular degradation of PGE_2 (Schuster, 2002) and/or a decrease in the de novo synthesis of PGE_2 as a result of attenuated Cox-2 expression in mrp4-deficient cells. Similar results were also obtained using the approach of RNA interference-mediated knockdown of mrp4 in wild-type cells. Mrp4 knockdown produces a relatively smaller reduction in basal Cox-2 levels than that occurring in *mrp4*$^{-/-}$ cells because the depletion of mrp4 by this approach is only partial. For the same reason, the intracellular PGE_2 levels may be less affected compared with those occurring in *mrp4*$^{-/-}$ cells. Collectively, the findings suggest that mrp4 functions as a major efflux transporter for PGE_2 and a mechanism for regulating PGE_2 synthesis in MEF cells. The reduction in Cox-2 expression occurs secondarily to the absence of mrp4, presumably serving to prevent the build-up of intracellular PGE_2 and/or excessive PGE_2 synthesis. The inter-play between MRP4 and prostaglandin-synthesizing enzymes has been suggested by the recent report of Rius et al. (2005) demonstrating that MRP4 and Cox-2 are coexpressed and colocalized in epithelia cells of the human seminal vesicles, a source of prostaglanoids, in the

urogenital tract. This finding substantiates our assertion that mrp4 is indispensable for cells actively producing and secreting prostaglandins.

Consistent with the consequences of an mrp4 deficiency in vitro, *mrp4*$^{-/-}$ mice display an approximate 50% decrease in the plasma level of the PGE metabolite. Mrp2 may be responsible for the remaining 50% plasma level of PGE metabolite produced by mrp4 deficient mice. With respect to tissue distribution, MRP4 is reportedly expressed in the apical membrane of the proximal tubule of the kidney at a high level (van Aubel et al., 2002; Maher et al., 2005). Thus, the notion was that *mrp4*$^{-/-}$ mice should manifest an increase in the plasma PGE metabolite level because of impaired renal excretion. This contradiction to our finding may be reconciled by the assumption that the renal clearance of PGE metabolite still occurs possibly due to compensation by mrp2 in the kidney. In addition, the overall PGE synthesis and/or secretion by tissues of *mrp4*$^{-/-}$ mice is reduced. It has been broadly recognized that NSAIDs exert analgesic effects by inhibiting prostaglandin synthesis and preventing the lowering of the nociceptive threshold at both peripheral and central sites (Dionne et al., 2001; Burian and Geisslinger, 2005). Moreover, recent reports demonstrate that mrp4 is inhibited by indomethacin and several other NSAIDs at physiologically relevant concentrations (Reid et al., 2003; El-Sheikh et al., 2007). Therefore, the reduction in plasma PGE metabolite levels in *mrp4*$^{-/-}$ mice is likely to cause the phenotype of an increase in nociceptive thresholds in response to mechanical and thermal stimuli. Our findings provide the first evidence that mrp4-mediated prostaglandin transport has physiological significance in the regulation of inflammatory nociceptive responses in vivo. However, we cannot rule out a possible contribution of altered ion channel activity by PKA in nociceptive neurons (Fitzgerald et al., 1999) to the attenuation of pain responses in *mrp4*$^{-/-}$ mice. cAMP and cAMP agonists have been implicated in promoting PGE_2-induced primary afferent hyperalgesia (Taiwo et al., 1989). Because mrp4 deficiency causes the attenuation of PKA activity and Cox-2 expression in vitro, the involvement of the cAMP-mediated signaling pathway in modulating inflammatory nociceptive responses in vivo will be worthy of further investigation.

Acknowledgments

This work was supported in part by National Institute of Child Health and Human Development grant HD39997.

ABBREVIATIONS

MRP/mrp	human/murine multidrug resistance protein
MEF	mouse embryonic fibroblast
PMEA	9-(2-phosphonylmethoxyethyl)adenine
PG	prostaglandin
PKA	cAMP-dependent protein kinase
CRE	cAMP-response element
CREB	cAMP-response element-binding protein
Cox	cyclooxygenase
NSAID	nonsteroidal anti-inflammatory drug
kb	kilobase pair(s)
bp	base pair(s)

RT-PCR	reverse tranascription-polymerase chain reaction
MTS	3-(4,5-dimethylthiazol-2-yl)-5-(3-carboxymethoxyphenyl)-2-(4-sulfophenyl)-2*H*-tetrazolium, inner salt
EIA	enzyme immunoassay
PGEM	PGE_2 metabolite
shRNA	short hairpin RNA
FSK	forskolin
IBMX	3-isobutyl-1-methylxanthine
H-89	*N*-[2-(*p*-bromocinnamylamino)ethyl]-5-isoquinolinesulfonamide
ANOVA	analysis of variance
siRNA	short interfering RNA

References

Adachi M, Reid G, Schuetz JD. Therapeutic and biological importance of getting nucleotides out of cells: a case for the ABC transporters, MRP4 and 5. Adv Drug Deliv Rev 2002;54:1333–1342. [PubMed: 12406648]

Belinsky MG, Guo P, Lee K, Zhou F, Kotova E, Grinberg A, Westphal H, Shchaveleva I, Klein-Szanto A, Gallo JM, et al. Multidrug resistance protein 4 protects bone marrow, thymus, spleen, and intestine from nucleotide analogue-induced damage. Cancer Res 2007;67:262–268. [PubMed: 17210706]

Borst P, Balzarini J, Ono N, Reid G, de Vries H, Wielinga P, Wijnholds J, Zelcer N. The potential impact of drug transporters on nucleoside-analog-based antiviral chemotherapy. Antiviral Res 2004;62:1–7. [PubMed: 15026196]

Burian M, Geisslinger G. COX-dependent mechanisms involved in the antinociceptive action of NSAIDs at central and peripheral sites. Pharmacol Ther 2005;107:139–154. [PubMed: 15993252]

Chaplan SR, Bach FW, Pogrel JW, Chung JM, Yaksh TL. Quantitative assessment of tactile allodynia in the rat paw. J Neurosci Methods 1994;53:55–63. [PubMed: 7990513]

Chasin M, Harris DN. Inhibitory and activators of cyclic nucleotide phosphodiesterase. Adv Cyclic Nucleotide Res 1976;7:225–264. [PubMed: 188316]

Chen ZS, Guo Y, Belinsky MG, Kotova E, Kruh GD. Transport of bile acids, sulfated steroids, estradiol 17-*β*-D-glucuronide, and leukotriene C4 by human multidrug resistance protein 8 (ABCC11). Mol Pharmacol 2005;67:545–557. [PubMed: 15537867]

Chen ZS, Lee K, Kruh GD. Transport of cyclic nucleotides and estradiol 17-*β*-D-glucuronide by multidrug resistance protein 4. Resistance to 6-mercapto-purine and 6-thioguanine. J Biol Chem 2001;276:33747–33754. [PubMed: 11447229]

Chen ZS, Lee K, Walther S, Raftogianis RB, Kuwano M, Zeng H, Kruh GD. Analysis of methotrexate and folate transport by multidrug resistance protein 4 (ABCC4): MRP4 is a component of the methotrexate efflux system. Cancer Res 2002;62:3144–3150. [PubMed: 12036927]

Chijiwa T, Mishima A, Hagiwara M, Sano M, Hayashi K, Inoue T, Naito K, Toshioka T, Hidaka H. Inhibition of forskolin-induced neurite outgrowth and protein phosphorylation by a newly synthesized selective inhibitor of cyclic AMP-dependent protein kinase, *N*-[2-(*p*-bromocinnamylamino)ethyl]-5-isoquinolinesulfonamide (H-89), of PC12D pheochromocytoma cells. J Biol Chem 1990;265:5267–5272. [PubMed: 2156866]

de Waart DR, Paulusma CC, Kunne C, Oude Elferink RP. Multidrug resistance associated protein 2 mediates transport of prostaglandin E2. Liver Int 2006;26:362–368. [PubMed: 16584400]

Deeley RG, Westlake C, Cole SP. Transmembrane transport of endo- and xenobiotics by mammalian ATP-binding cassette multidrug resistance proteins. Physiol Rev 2006;86:849–899. [PubMed: 16816140]

Dionne RA, Khan AA, Gordon SM. Analgesia and COX-2 inhibition. Clin Exp Rheumatol 2001;19(6 Suppl 25):S63–S70. [PubMed: 11695255]

Dirig DM, Salami A, Rathbun ML, Ozaki GT, Yaksh TL. Characterization of variables defining hindpaw withdrawal latency evoked by radiant thermal stimuli. J Neurosci Methods 1997;76:183–191. [PubMed: 9350970]

Dixon WJ. Efficient analysis of experimental observations. Annu Rev Pharmacol Toxicol 1980;20:441–462. [PubMed: 7387124]

El-Sheikh AA, van den Heuvel JJ, Koenderink JB, Russel FG. Interaction of nonsteroidal anti-inflammatory drugs with multidrug resistance protein (MRP) 2/ABCC2- and MRP4/ABCC4-mediated methotrexate transport. J Pharmacol Exp Ther 2007;320:229–235. [PubMed: 17005917]

Fitzgerald EM, Okuse K, Wood JN, Dolphin AC, Moss SJ. cAMP-dependent phosphorylation of the tetrodotoxin-resistant voltage-dependent sodium channel SNS. J Physiol 1999;516:433–446. [PubMed: 10087343]

Guo Y, Kotova E, Chen ZS, Lee K, Hopper-Borge E, Belinsky MG, Kruh GD. MRP8, ATP-binding cassette C11 (ABCC11), is a cyclic nucleotide efflux pump and a resistance factor for fluoropyrimidines 2′,3′-dideoxycytidine and 9′-(2′-phosphonylmethoxyethyl)adenine. J Biol Chem 2003;278:29509–29514. [PubMed: 12764137]

Jedlitschky G, Burchell B, Keppler D. The multidrug resistance protein 5 functions as an ATP-dependent export pump for cyclic nucleotides. J Biol Chem 2000;275:30069–30074. [PubMed: 10893247]

Kruh GD, Belinsky MG. The MRP family of drug efflux pumps. Oncogene 2003;22:7537–7552. [PubMed: 14576857]

Lee K, Klein-Szanto AJ, Kruh GD. Analysis of the MRP4 drug resistance profile in transfected NIH3T3 cells. J Natl Cancer Inst 2000;92:1934–1940. [PubMed: 11106685]

Lin ZP, Belcourt MF, Carbone R, Eaton JS, Penketh PG, Shadel GS, Cory JG, Sartorelli AC. Excess ribonucleotide reductase R2 subunits coordinate the S phase checkpoint to facilitate DNA damage repair and recovery from replication stress. Biochem Pharmacol 2007;73:760–772. [PubMed: 17188250]

Lin ZP, Johnson DR, Finch RA, Belinsky MG, Kruh GD, Sartorelli AC. Comparative study of the importance of multidrug resistance-associated protein 1 and P-glycoprotein to drug sensitivity in immortalized mouse embryonic fibroblasts. Mol Cancer Ther 2002;1:1105–1114. [PubMed: 12481434]

Maher JM, Cheng X, Slitt AL, Dieter MZ, Klaassen CD. Induction of the multidrug resistance-associated protein family of transporters by chemical activators of receptor-mediated pathways in mouse liver. Drug Metab Dispos 2005;33:956–962. [PubMed: 15833929]

Mayr B, Montminy M. Transcriptional regulation by the phosphorylation-dependent factor CREB. Nat Rev Mol Cell Biol 2001;2:599–609. [PubMed: 11483993]

Meade EA, Smith WL, DeWitt DL. Differential inhibition of prostaglandin endoperoxide synthase (cyclooxygenase) isozymes by aspirin and other non-steroidal anti-inflammatory drugs. J Biol Chem 1993;268:6610–6614. [PubMed: 8454631]

Pino MS, Nawrocki ST, Cognetti F, Abruzzese JL, Xiong HQ, McConkey DJ. Prostaglandin E2 drives cyclooxygenase-2 expression via cyclic AMP response element activation in human pancreatic cancer cells. Cancer Biol Ther 2005;4:1263–1269. [PubMed: 16319525]

Reid G, Wielinga P, Zelcer N, van der Heijden I, Kuil A, de Haas M, Wijnholds J, Borst P. The human multidrug resistance protein MRP4 functions as a prostaglandin efflux transporter and is inhibited by nonsteroidal antiinflammatory drugs. Proc Natl Acad Sci U S A 2003;100:9244–9249. [PubMed: 12835412]

Rius M, Thon WF, Keppler D, Nies AT. Prostanoid transport by multidrug resistance protein 4 (MRP4/ABCC4) localized in tissues of the human urogenital tract. J Urol 2005;174:2409–2414. [PubMed: 16280858]

Sauna ZE, Nandigama K, Ambudkar SV. Multidrug resistance protein 4 (ABCC4)-mediated ATP hydrolysis: effect of transport substrates and characterization of the post-hydrolysis transition state. J Biol Chem 2004;279:48855–48864. [PubMed: 15364914]

Schuetz JD, Connelly MC, Sun D, Paibir SG, Flynn PM, Srinivas RV, Kumar A, Fridland A. MRP4: A previously unidentified factor in resistance to nucleoside-based antiviral drugs. Nat Med 1999;5:1048–1051. [PubMed: 10470083]

Schuster VL. Prostaglandin transport. Prostaglandins Other Lipid Mediat 2002;68–69:633–647.

Seamon KB, Padgett W, Daly JW. Forskolin: unique diterpene activator of adenylate cyclase in membranes and in intact cells. Proc Natl Acad Sci U S A 1981;78:3363–3367. [PubMed: 6267587]

Shimizu H, Taniguchi H, Hippo Y, Hayashizaki Y, Aburatani H, Ishikawa T. Characterization of the mouse Abcc12 gene and its transcript encoding an ATP-binding cassette transporter, an orthologue of human ABCC12. Gene 2003;310:17–28. [PubMed: 12801629]

Smith WL, DeWitt DL, Garavito RM. Cyclooxygenases: structural, cellular, and molecular biology. Annu Rev Biochem 2000;69:145–182. [PubMed: 10966456]

Taiwo YO, Bjerknes LK, Goetzl EJ, Levine JD. Mediation of primary afferent peripheral hyperalgesia by the cAMP second messenger system. Neuroscience 1989;32:577–580. [PubMed: 2557557]

van Aubel RA, Smeets PH, Peters JG, Bindels RJ, Russel FG. The MRP4/ABCC4 gene encodes a novel apical organic anion transporter in human kidney proximal tubules: putative efflux pump for urinary cAMP and cGMP. J Am Soc Nephrol 2002;13:595–603. [PubMed: 11856762]

Wardlaw SA, Zhang N, Belinsky SA. Transcriptional regulation of basal cyclooxygenase-2 expression in murine lung tumor-derived cell lines by CCAAT/enhancer-binding protein and activating transcription factor/cAMP response element-binding protein. Mol Pharmacol 2002;62:326–333. [PubMed: 12130685]

Wielinga PR, van der Heijden I, Reid G, Beijnen JH, Wijnholds J, Borst P. Characterization of the MRP4- and MRP5-mediated transport of cyclic nucleotides from intact cells. J Biol Chem 2003;278:17664–17671. [PubMed: 12637526]

Wijnholds J, Mol CA, van Deemter L, de Haas M, Scheffer GL, Baas F, Beijnen JH, Scheper RJ, Hatse S, De Clercq E, et al. Multidrug-resistance protein 5 is a multispecific organic anion transporter able to transport nucleotide analogs. Proc Natl Acad Sci U S A 2000;97:7476–7481. [PubMed: 10840050]

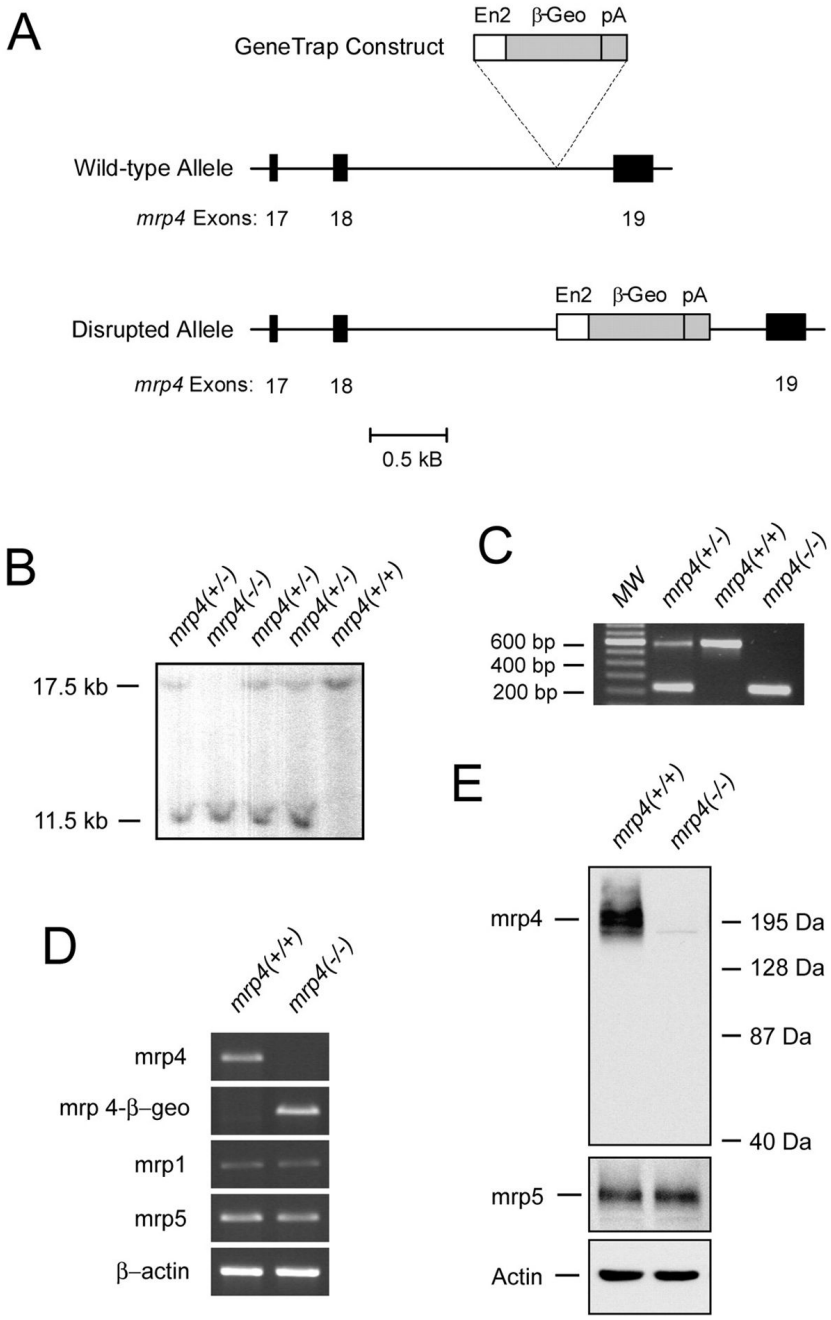

Fig. 1.

Identification of mice with homozygous disruption of the *mrp4* gene and expression of *mrp4* in derived immortalized MEF cells. A, partial maps of the mouse genomic *mrp4* locus, the GeneTrap construct, and the disrupted allele. Exons 17, 18, and 19 of the *mrp4* gene are shown as solid bars. The GeneTrap construct was inserted into the intronic sequence between exons 18 and 19 of the *mrp4* gene. The size of the GeneTrap construct was not drawn to scale. En2, the mouse En2 intron 1 containing a splice acceptor of the En2 exon 2 preceding the *β*-geo exon. *β*-geo, fusion of *β*-galactosidase and neomycin transferase. pA, simian virus 40 polyadenylation signal. B, southern blot analysis of the *mrp4* locus in mice. Tail genomic DNA was digested with EcoRV, and the blot was hybridized with a 514 bp of ^{32}P-labeled probe

located 5′ to the disrupted intronic sequence of *mrp4*. The wild-type band is 17.5 kb; the insertion results in a band of 11.5 kb. C, PCR genotyping for disruption of the *mrp4* locus in mice. MW, molecular size marker. Five nanograms of genomic DNA was amplified by PCR with a cocktail of three primers as described under *Materials and Methods*. The reaction yielded a 582-bp wild-type product and a 220-bp knockout product that were separated on an agarose gel stained with ethidium bromide. (D) RT-PCR analysis of the mrp4 transcript in MEF cells. Total RNA from $mrp4^{+/+}$ and $mrp4^{-/-}$ MEF cells was reverse-transcribed and amplified with primer sets specific for mrp4, mrp4/β-geo fusion, mrp1, mrp5, and β-actin cDNAs. PCR products were separated on an agarose gel stained with ethidium bromide. E, Western blot analysis of mrp4 protein expression in MEF cells. Total protein was analyzed for mrp4, mrp5, and actin. Actin protein was used to demonstrate approximately equal loading of each lane.

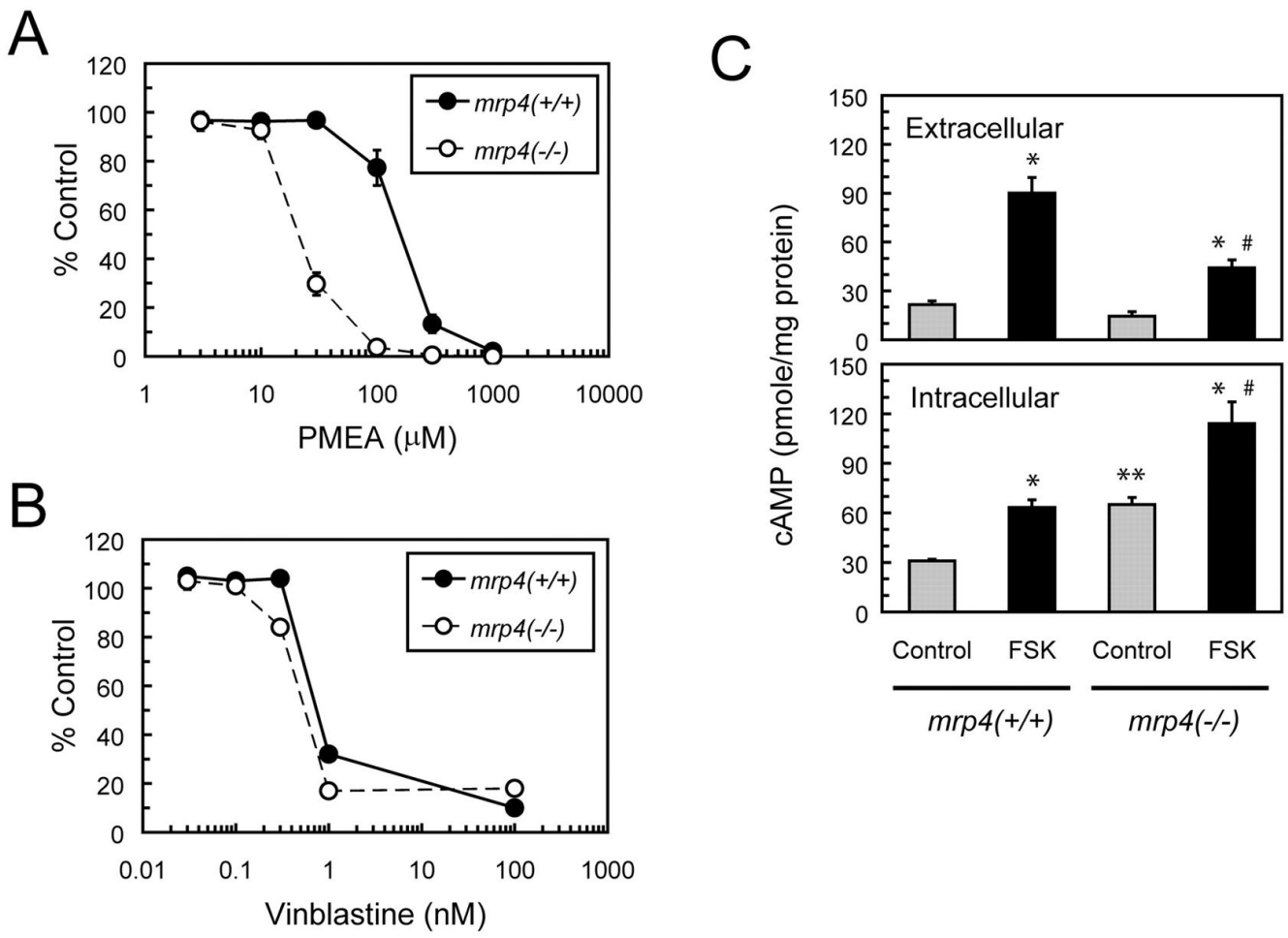

Fig. 2.

Effects of mrp4 deficiency on the intracellular accumulation of PMEA and cyclic AMP in MEF cells. A and B, cytotoxicities of PMEA and vinblastin. *Mrp4*$^{+/+}$ and *mrp4*$^{-/-}$ MEF cells were exposed to various concentrations of PMEA or vinblastine for 72 h. Cell viability was then determined by the MTS cytotoxicity assay and expressed as a percentage of a vehicle-treated control. Data points are the mean ± S.E. of three determinations. C, extracellular and intracellular levels of cAMP. After 24 h of culture under normal conditions, *mrp4*$^{+/+}$ and *mrp4*$^{-/-}$ MEF cells were treated with vehicle or 10 μM FSK for 1 h. The growth medium and cellular extracts were collected and assayed for cAMP levels using an EIA kit as described under *Materials and Methods*. Both extracellular and intracellular levels of cAMP were normalized against the amount of intracellular protein for respective samples and expressed as picomoles per milligram of protein. Values are the mean ± S.E. of three determinations. Statistical difference was determined by a one-way ANOVA. *, $p < 0.05$, compared with the control in each genotype. **, $p < 0.05$, compared with control *mrp4*$^{+/+}$ MEF cells. #, $p < 0.05$, compared with FSK-treated *mrp4*$^{+/+}$ MEF cells.

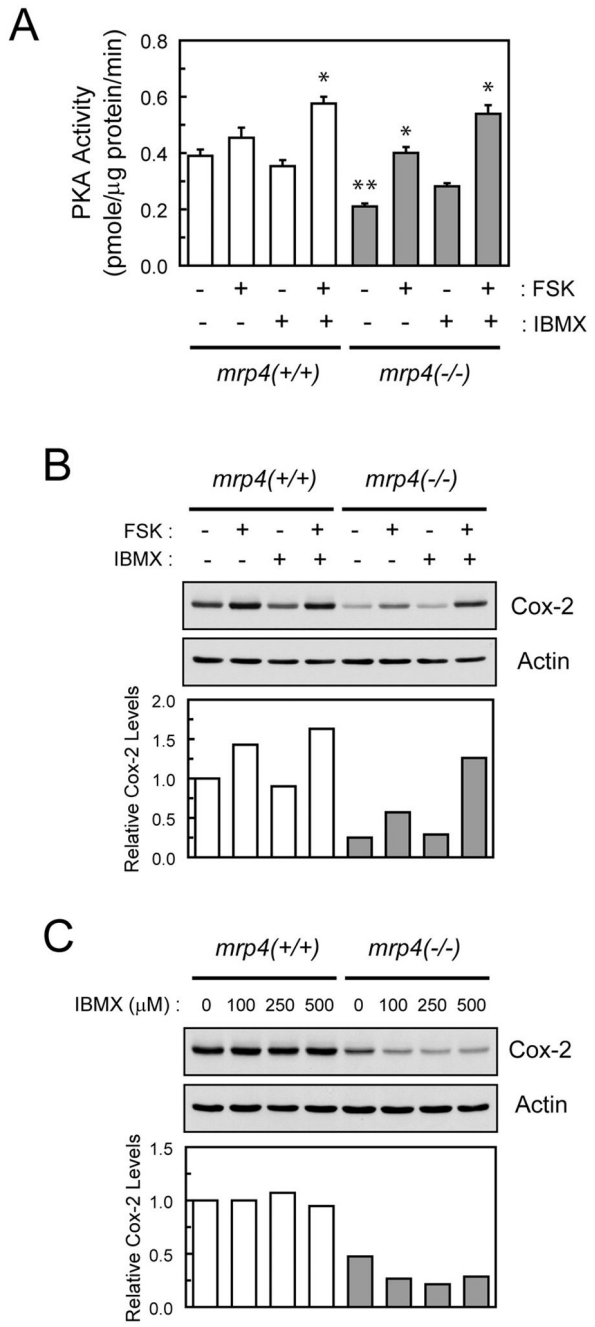

Fig. 3.

Effects of mrp4 deficiency on PKA activity and Cox-2 expression in MEF cells. A, PKA activity in MEF cells exposed to FSK and IBMX. *Mrp4*$^{+/+}$ and *mrp4*$^{-/-}$ MEF cells were plated for 24 h and then treated with 250 μM IBMX for 30 min before treatment with 10 μM FSK for 1 h. Cellular extracts were prepared for determination of PKA activity as described under *Materials and Methods*. PKA activity is expressed as picomoles per minute per microgram of total protein. Values are the mean ± S.E. of three determinations. Statistical difference was determined by a one-way ANOVA. *, $p < 0.05$, compared with the control in each genotype. **, $p < 0.05$, compared with control *mrp4*$^{+/+}$ MEF cells. B, Cox-2 expression in MEF cells exposed to FSK and IBMX. After plating for 24 h, *mrp4*$^{+/+}$ and *mrp4*$^{-/-}$ MEF cells were

pretreated with 250 μM IBMX for 30 min and then exposed to vehicle or 10 μM FSK for 6 h. Forty micrograms of total protein were analyzed for Cox-2 and actin levels by Western blotting. Quantification of Cox-2 protein levels is shown as the ratio of Cox-2 to actin for respective samples. C, effects of prolonged exposure to IBMX on Cox-2 expression. *Mrp4*$^{+/+}$ and *mrp4*$^{-/-}$ MEF cells were plated and simultaneously treated with various concentrations of IBMX for 24 h. Total protein was analyzed for Cox-2 levels as described in B.

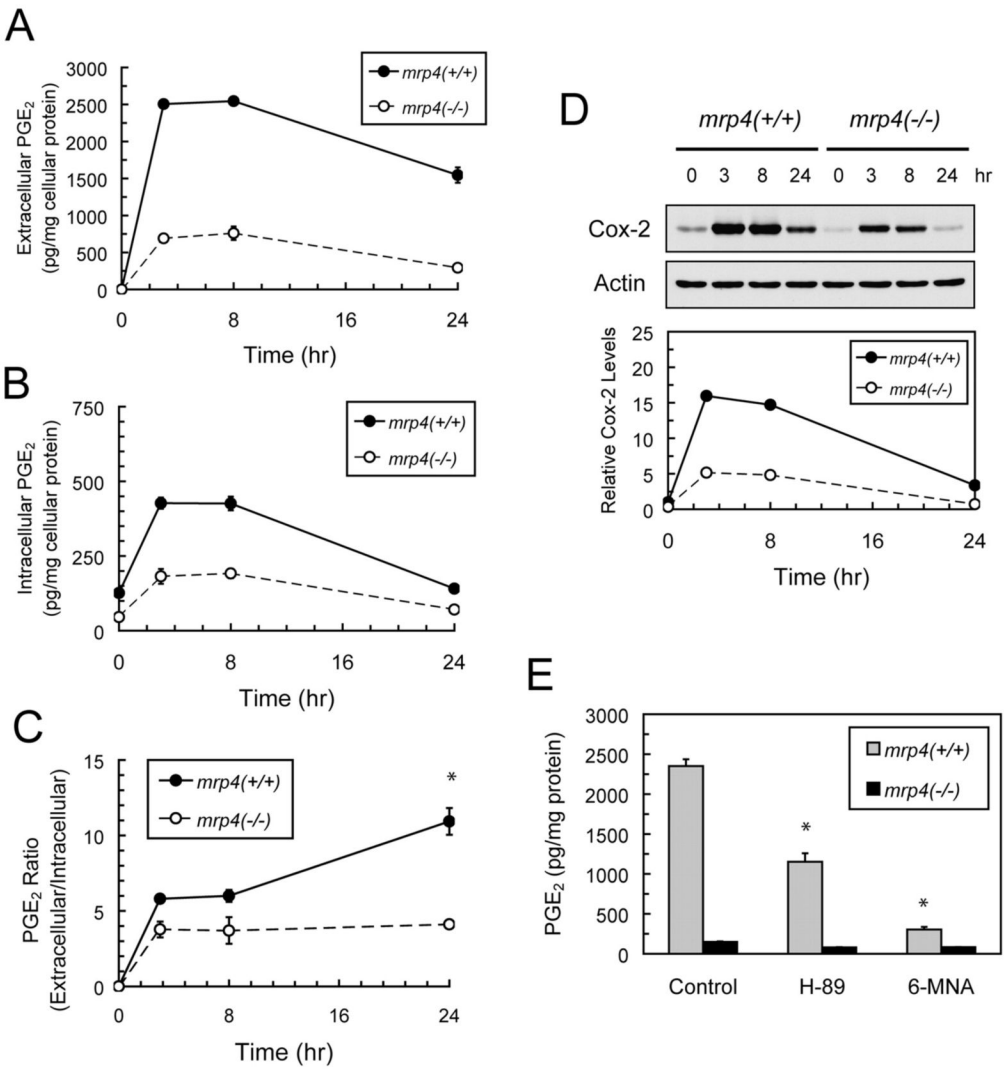

Fig. 4.

Effects of mrp4 deficiency on the transport of PGE_2 in MEF cells. A and B, time courses of extracellular and intracellular levels of PGE_2 after plating of MEF cells. After cell plating, the growth medium and cell pellets of *mrp4*$^{+/+}$ and *mrp4*$^{-/-}$ MEF cells were collected at the indicated time points. The medium and purified cell lysates were assayed for the concentrations of extracellular and intracellular PGE_2 using an EIA kit as described under *Materials and Methods*. The values were the means ± S.E. from measurements of three independent wells performed in a single experiment. C, time-dependent changes in the ratio of extracellular to intracellular PGE_2 levels. The calculated ratios were based on the PGE_2 levels presented in A and B. *, $p < 0.05$, compared with mrp4$^{-/-}$ MEF cells at each time point; unpaired *t* test, two-tail. D, the time course of Cox-2 induction after plating of MEF cells. Aliquots of cells from the treatment described in A and B were collected and analyzed for the protein levels of Cox-2 and actin by Western blotting. The relative Cox-2 level was obtained by normalizing the Cox-2 level against the actin level at each time point. E, effects of PKA and Cox-2 inhibitors on extracellular PGE_2 levels. *Mrp4*$^{+/+}$ and *mrp4*$^{-/-}$ MEF cells were plated and grown in the absence and presence of 10 μM H-89 or 50 μM 6-methoxy-2-naphthyl acetic acid for 24 h. The growth medium was collected and assayed for PGE_2 levels. Levels of PGE_2 are expressed as picograms per milligram of cellular protein. Data are the means ± S.E. from measurements of

three independent wells performed in each of two independent experiments. Statistical difference was determined by a one-way ANOVA. *, $p < 0.05$, compared with the control in each genotype.

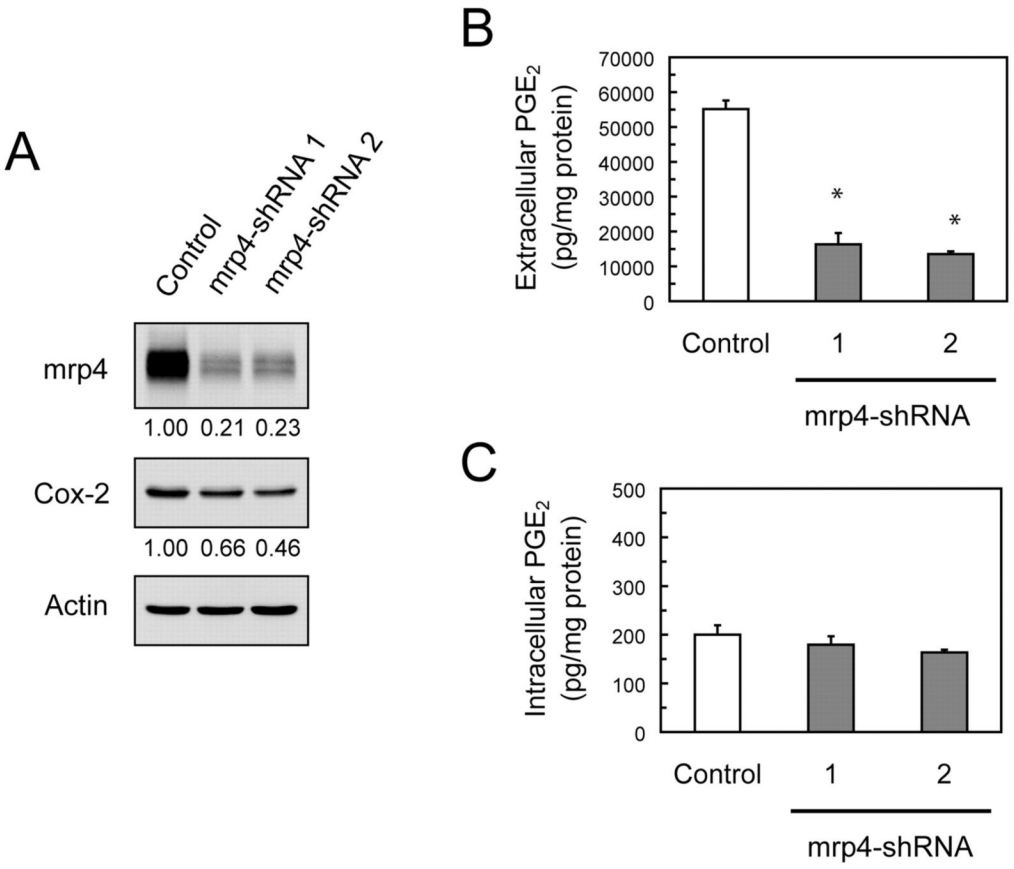

Fig. 5.

Effects of mrp4 knockdown on the levels of Cox-2 and PGE_2 in wild-type MEF cells. A, siRNA-mediated knockdown of mrp4 in *mrp4*$^{+/+}$ MEF cells. *Mrp4*$^{+/+}$ MEF cells were transfected with the nontarget sequence shRNA (control), mrp4-shRNA 1, or mrp4-shRNA 2 and then grown for 72 h. Total protein was isolated from cells and analyzed for mrp4, Cox-2, and actin protein by Western blotting, with relative quantitative levels of mrp4 and Cox-2 given below the blots. B and C, Levels of extracellular and intracellular PGE_2 in mrp4-knockdown MEF cells. After 48 h of transfection as described in A, the growth medium was removed and replaced with fresh complete medium and cells were grown for another 24 h. The medium and purified cell lysates were assayed for the levels of extracellular and intracellular PGE_2, respectively; the levels of PGE_2 are expressed as picograms per milligram of cellular protein. Data are the mean ± S.E. of three determinations. Statistical difference was determined by a one-way ANOVA. *, $p < 0.05$, compared with cells transfected with the control shRNA.

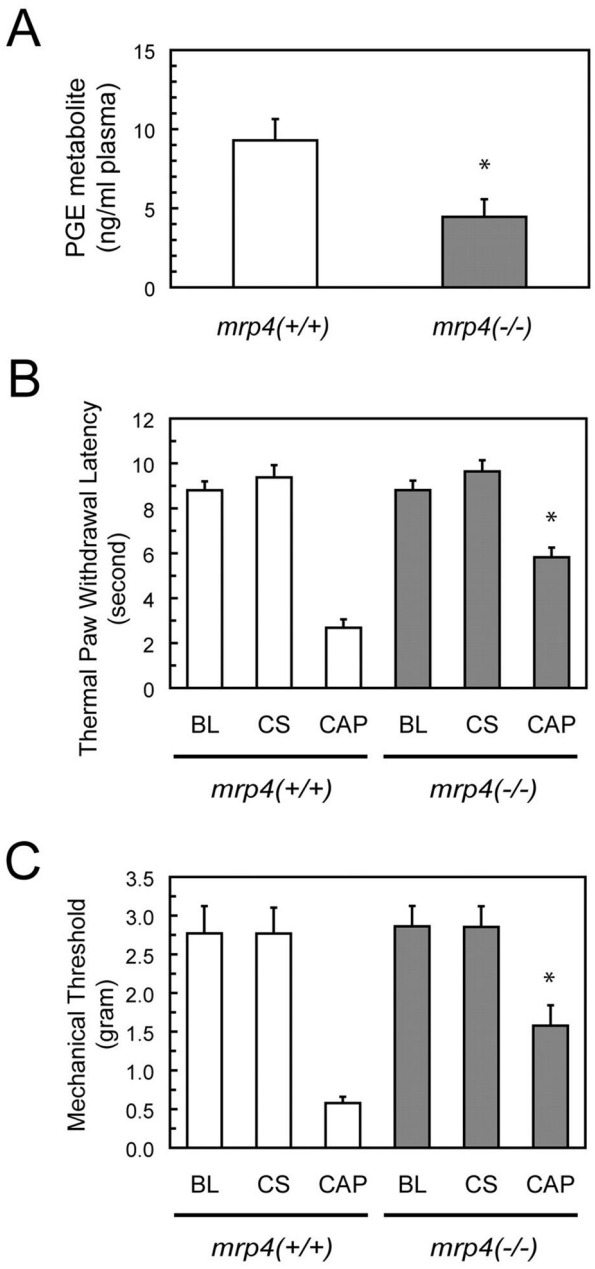

Fig. 6.

Plasma PGE levels and nociceptive responses of mrp4 deficient mice. A, plasma levels of PGE metabolite in mice. Peripheral blood was collected from *mrp4*$^{+/+}$ and *mrp4*$^{-/-}$ mice. The plasma was then obtained for measurements of PGE metabolite levels. PGE metabolite levels are expressed as nanograms per milliliter of plasma. Values are the mean ± S.E. from determinations of six to seven mice per each genotype. *, $p < 0.05$, compared with wild-type mice; unpaired *t* test, two-tail. B and C, thermal paw withdrawal latency and mechanical sensory thresholds in mice. Capsaicin was injected into the left hind paws (CAP) of *mrp4*$^{+/+}$ and *mrp4*$^{-/-}$ mice 30 min before tests. As a negative control, the right hind paws (control side, CS) of the same mice were not injected with capsaicin. The duration of thermal paw withdrawal and the mechanical sensory threshold were measured as described under *Materials and*

Methods and expressed in seconds and grams, respectively. Mice not injected with capsaicin were used to determine the baseline (BL) of thermal and mechanical thresholds. All values are the mean ± S.E. of determinations performed with three to eight animals. *, $p < 0.05$, compared with wild-type mice; unpaired *t* test, two-tail.